Research Journal of Applied Sciences 9 (6): 299-307, 2014
ISSN: 1815-932X
© Medwell Journals, 2014

Automatic Computer Aided Diagnosis System for Detection of Lung Cancer Nodules Using Region Growing Method and Support Vector Machines (SVM)

[1]S. Shaik Parveen and [2]C. Kavitha
[1]Bharathiar University, Coimbatore, Tamil Nadu, India
[2]Department of Computer Science, Thiruvalluvar Government Arts College, Rasipuram, India

Abstract: Lung cancer is considered to be the main cause of cancer death worldwide and it is difficult to detect in its early stages because symptoms appear only in the advanced stages causing the mortality rate to be the highest among all other types of cancer. So, the early detection of cancer is vital to cure the disease completely. Many Computer Aided Detection Systems arise to increase the accuracy and performance rate. But still the performance rate is not high. This study proposes a complete automatic Computer Aided Diagnosis System (CAD) for early detection of lung cancer nodules using Chest Computer Tomography (CT) scan images. The proposed method consists of four phases. They are lung extraction, segmentation of lung region, feature extraction and finally classification of normal, benign and malignancy in the lung. Threat pixel identification with region growing method is used for segmentation of focal areas in the lung. For feature extraction Gray Level Co-occurrence Matrix (GLCM) and Gabor features are used. Extracted features are classified using Support Vector Machine (SVM). The experimentation is performed with the help of real time computer tomography images. The proposed algorithm is fully automatic and has shown 100% sensitivity.

Key words: Computer tomography, computer aided detection, threat pixel identification, region growing method, support vector machine

INTRODUCTION

Lung cancer is considered to be the main cause of cancer death worldwide and it is difficult to detect in its early stages because symptoms appear only in the advanced stages causing the mortality rate to be the highest among all other types of cancer. More people die because of lung cancer than any other types of cancer such as breast, colon and prostate cancers. There is significant evidence indicating that the early detection of lung cancer will decrease mortality rate. The most recent estimates according to the latest statistics provided by world health organization indicates that around 7.6 million deaths worldwide each year because of this type of cancer. Furthermore, mortality from cancer are expected to continue rising to become around 17 million worldwide in 2030. Early detection of lung cancer is valuable. The 5 years survival rate of lung cancer has stagnated in the last 30 years and is now at approximately just 15%. Lung cancer takes more victims than breast cancer, prostate cancer and colon cancer together. This is due to the asymptomatic growth of this cancer. In the majority of cases it is too late for a successful therapy if the patient develops first symptoms (e.g., chronic croakiness or hemoptysis). But if the lung cancer is detected early (mostly by chance), there is a survival rate at 47% according to the American Cancer Society.

The Chest Computed Tomography (CT) images are difficult in diagnostic imaging modality for the detection of lung cancer and the resolution of any equivocal abnormalities detected on chest radiographs (Howe and Gross, 1987). In particular, the expanding volume of thoracic CT studies along with the increase of image data, bring in focus the need for CAD algorithms to assist the radiologists (Abe *et al*., 2004). A variety of computer assisted detection techniques have been proposed. In the development of CAD System, it involves two main categories such as Computer Aided Detection (CADe) and Computer Aided Diagnosis (CADi). The construction of CAD System would increase the mortality rate and reduce the unnecessary biopsies in patients with benign case and thus prevent physical and mental depression of patients. Thus, CAD acts as a second reader and assists radiologist for accurate and efficient detection of cancer cells in the earlier stages. Thus, the radiologist use CAD scheme to improve the detection accuracy.

Previous research: There are many CAD Systems are proposed earlier for the detection of lung cancer nodules and for the diagnosis.

Corresponding Author: C. Kavitha, Department of Computer Science, Thiruvalluvar Government Arts College, Rasipuram, India

Suzuki *et al.* (2006) proposed a different technique using Massive Training Artificial Neural Networks (MTANN). It gives a new idea and remedy to the problem when the lung nodules overlap with the ribs or clavicles in chest radiographs faced by radiologists as well as Computer-Aided Diagnostic (CAD) Systems to detect these nodules. An MTANN is a non-linear filter that can be trained by use of input chest radiographs and the equivalent teaching images. They used a linear-output Back-Propagation (BP) algorithm that was derived for the linear-output multilayer ANN Model in order to train the MTANN. The dual-energy subtraction is a technique used for separating bones from soft tissues in chest radiographs by using the energy dependence of the x-ray attenuation by different materials.

Using fuzzy rules (Lee *et al.*, 2001) proposed a Template-matching technique based on Genetic Algorithms (GA) Template Matching (GATM) for detection of nodules existing within the lung area. In their research, GA was used to determine the target position in the observed image efficiently and to select an adequate template image from several reference patterns for quick template matching.

Kim *et al.* (2007) proposed a three step segmentation process for the analysis of lung image. In their approach, if the area in the CT image occupied by GGO is large then it is easy for a medical doctor to extract the features. However, the possibility to overlook the light gray shadow becomes higher when GGO exists as a small area. In the first step of their model, extracting ROI is performed to segment the lung area. To achieve better segmentation accuracy, preprocessing the CT slices is carried out by employing binarization, labeling, shrinking and expansion. In the second step, calculation of characteristics of GGO shadows such as mean value, standard deviation and semi interquartile range have been carried out. In the final step, the GGO shadow's regions were extracted by linear discriminant function. Suspicious shadows are extracted by Variable N-Quoit (VNQ) filter from GGO. The suspicious shadows are classified into a certain number of classes using feature values calculated from the suspicious shadows.

Dougherty *et al.* (2003) presented a temporal registration of CT scans of the lung. Their approach is based on an optical flow method and assumes a certain measure of intensity correspondence that scans containing pathology do not exhibit.

Penedo *et al.* (1998) described a computer-aided diagnosis scheme which has two-level Artificial Neural Network (ANN) architecture. In first level artificial neural network identifies suspicious regions in a low-resolution image. The curvature peaks calculated for all pixels in each suspicious region is given as the input to the second artificial neural network. The small size tumors are identified by the signature in curvature-peak feature space where curvature is the local curvature of the image data when sighted as a relief map. The result gives a true positive identification in this network is threshold at a particular level of importance.

Okada *et al.* (2005) proposed a multiscale joint segmentation and model fitting solution which extends the robust mean shift-based analysis to the Linear Scale-Space Theory. In their study, an ellipsoidal (anisotropic) geometrical structure of pulmonary nodules in the multislice X-ray Computed Tomography (CT) images was used for target's center location, ellipsoidal boundary approximation, volume, maximum/average diameters.

Hu *et al.* (2001) used conventional region-based methods that implemented the concept of thresholding, region growing and component labeling and morphological processing. The automatic segmentation works on 3D CT volumes and is tested on data sets of 8 normal subjects that were scanned three times at biweekly intervals. They used this template to find the structures with similar properties of nodules. Sluimer *et al.* (2005) proposed a refined segmentation by registration scheme in which an atlas based segmentation of the pathological lungs is refined by applying voxel classification to the border volume of the transformed probabilistic atlas approach.

Song *et al.* (2012) presented a new method to automatically detect both tumors and abnormal lymph nodes based on the low-level intensity and neighborhood features and high-level contrast-type features with a two-level SVM classification. One level of Conditional Random Field (CRF) is based on unary level contextual and spatial features and pair wise-level spatial features. Other level is based by relabeling the detected tumors as positive or mediastinum by filtering the high-uptake myocardium areas.

Ye *et al.* (2009) presented a new Computer Tomography (CT) lung nodule Computer-Aided Detection (CAD) Method. The method can be implemented for detecting both solid nodules and Ground-Glass Opacity (GGO) nodules. Foremost step of the method is to segment the lung region from the CT data using a fuzzy thresholding technique. The next step is the calculation of the volumetric shape index map and the dot map. The former mentioned map is based on local Gaussian and mean curvatures and the later one is based on the eigen values of a Hessian matrix. They are calculated for each Voxel within the lungs to enhance objects of a specific shape with high spherical elements. The combination of

the shape index and dot features provides a good structure descriptor for the initial nodule candidate generation. Certain advantages like high detection rate, fast computation and applicability to different imaging conditions and nodule types make the method more reliable for clinical applications.

Pohle and Toennies (2001) suggest adaptive region growing for segmentation of medical images. In this study, region growing is discussed using automatic tools where the Region Growing algorithm learns its homogeneity criterion automatically from characteristics of the region to be segmented and it allows a segmentation of individual structures. By analyzing the materials (Parveen and Kavitha, 2012), researchers proposed Automatic Region Growing Method for segmentation, GLCM and Gabor features for feature extraction and SVM for classification for diagnosing the occurrence of lung cancer.

MATERIALS AND METHODS

The proposed system consists of four steps for the detection of lung cancer nodules. They are as follows:

- Extraction of lung region from Computer Tomography (CT) images with different preprocessing techniques
- Segmentation of lung region using threat pixel identification with Region Growing Method
- Feature extraction using Gray Level Co-occurrence Matrix (GLCM) and gabor features
- Classification to identify normal, benign and malignant cancer of the lung using Support Vector Machine (SVM)

Preprocessing techniques: The initial step of the proposed system is the extraction of lung region from thproce chest computer tomography scan image. Computer Tomography (CT) images are difficult to interpret. Preprocessing is essential to improve the quality of CT images. The image processing methods used for this phase are PSNR calculation, erosion, median filter, dilation, outlining, lung border extraction, flood fill algorithm and finally extraction of lung parenchyma. The preprocessing methods are shown in Fig. 1.

The first step is application of PSNR (Peak Signal to Noise Ratio) calculation to the CT scan images which is used fetch a single raw image from a bulk of sectional slices of a single patient. PSNR is most commonly used to measure of quality. Although, a higher PSNR generally

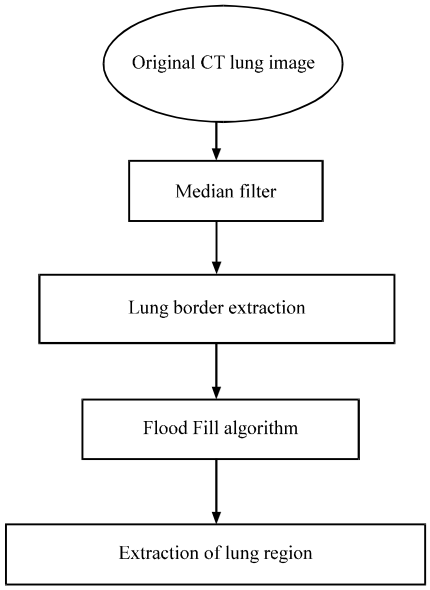

Fig. 1: Preprocessing methods using Computer Tomography (CT) images

indicates that the reconstruction is of higher quality. The best suitable with better accuracy is chosen for the further enhancement of lung region.

The Mean Square Error (MSE) and the Peak Signal to Noise Ratio (PSNR) are the two error metrics used to compare image compression quality. The MSE represents the cumulative squared error between the compressed and the original image whereas PSNR represents a measure of the peak error. The lower the value of MSE, the lower the error. To compute the PSNR, the block first calculates the Mean-Squared Error (MSE) using the following equation:

$$MSE = \frac{1}{mn}\sum_{i=0}^{m-1}\sum_{j=0}^{n-1}[I(i,j) - K(i,j)]^2 \quad (1)$$

In the equation, m and n are the number of rows and columns in the input images I and K, respectively. Then, the block computes the PSNR using the following equation: The PSNR is defined as:

$$PSNR = 10.\log_{10}\left(\frac{x^2}{MSE}\right) \quad (2)$$

Here, x^2 is the maximum fluctuation in the input image data type. The noise can be removed by using median filter. By applying the edge detection the lung region border is then obtained. Finally, to fill the obtained lung border with the lung region Flood Fill algorithm is used.

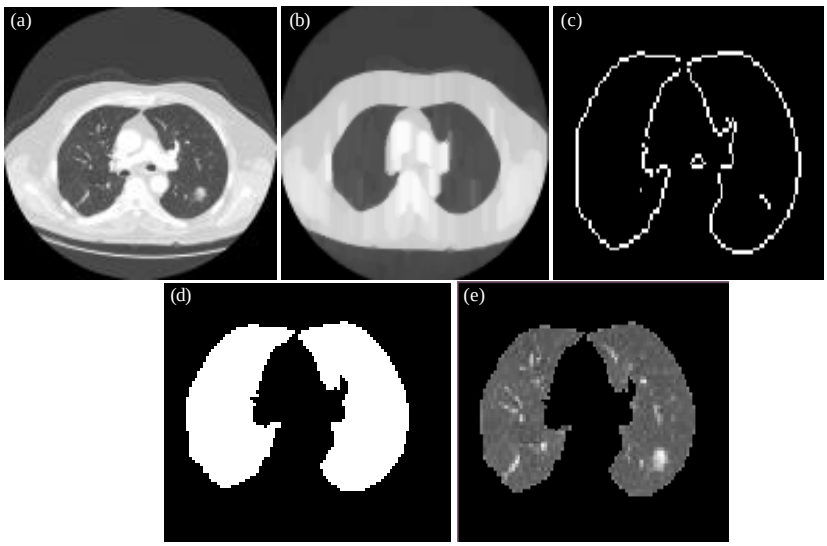

Fig. 2: Preprocessing methods for extraction of lung region; a) original image; b) filtered image (Median filter); c) border extraction; d) flood fill technique and e) lung region extraction

Finally, the lung region is extracted and used for the segmentation to detect the cancer nodule. Figure 2 shows the preprocessing techniques used in extracting the lung region from Computer Tomography (CT) scan images from a through e where Fig. 2e shows the extracted lung region.

Segmentation: The next step in Computer Aided Diagnosis System is segmentation. Image segmentation is a crucial step for any image processing technology. The aim of segmentation is to determine the focal area in the lung. This step will identify the Region of Interest (ROI) which helps in identifying the region of cancer in lung nodules. Many researchers have performed segmentation using region growing methodology. For example, Pohle and Toennies (2001) suggest adaptive region growing for segmentation of medical images. In this study, region growing is discussed using automatic tools where the Region Growing Algorithm learns its homogeneity criterion automatically from characteristics of the region to be segmented and it allows a segmentation of individual structures.

Yim *et al.* (2005) stated about hybrid lung segmentation in chest CT images for computer-aided diagnosis. The proposed system contains three phases. In the first phase, lungs and airways are separated by an inverse seeded region growing and linked component labeling. In the second phase, trachea and large airways are eliminated from the lungs by three-dimensional region growing. In the final phase, exact lung region borders are obtained by subtracting the outcome of the second phase from that of the first phase. But still the segmentation has to be improved for better accuracy. Bellotti *et al.* (2007) proposed a CAD System using region growing and Active Contour Model with detection rate 88.5% which is still has to be improved.

Conventional Region Growing algorithm: The RG is an image analysis technique that consists of searching for connected regions of pixels satisfying a given inclusion rule. The algorithm works as follows:

Step 1: A seed point is chosen and its neighbors are considered.

Step 2: If the neighbors satisfy the inclusion rule, they are included in the growing region, otherwise they are ruled out.

Step 3: All points included at a certain step become seed points for the following step.

Step 4: The routine is iterated until no more points satisfy the inclusion rule. The main problem of a RG algorithm relies in the selection of a proper seed point which is usually done by hand.

Automatic Region Growing Algorithim (ARGA): Automatic Region Growing Algorithm (ARGA) is used for segmentation. Selection of seed pixel depends mainly on the problem domain. To overcome this problem all the objects in an image are detected without any manual specification of the seed pixel in ARGA.

Threat pixel identification: Threat pixels are produced by thresholding the preprocessed image. Threat pixel threshold is determined by histogram analysis. Segmentation through threat pixel identification contains the following steps:

Step 1: Computation of histogram and accumulated histogram are done to get Hlc and AHlc.

Step 2: Location of peaks in Hlc is found by using histogram gradient changes (HP1, HP2, ..., HPi) where HPj are the gray levels.

Step 3: Threat threshold's candidates are selected by following condition, Tt = {Hpj|when the selected threat area ≤10% of the entire region of interest where j = 1, 2, …, i}, S = r, r + 1… z. AHlc can be used to calculate the selected threat area.

Step 4: Threat threshold should be among of {Ts; S = r~z} i.e., Tt = Tl r≤l≤z, such that |HPi-HPi-1| is maximum among {|Hpk-HPk-1|; S = r~z}.

Step 5: Pixel is marked at (u, v) as a candidate of threat pixel if p (u, v)>Tt by using Ti(u, v) = 4-y where y = 1, 2, 3.

Step 6: A pixel at (u, v) is considered as threat pixel if $\sum_{y=1}^{3} T_i(u, v) > 5$.

Region Growing Method: Region Growing Method seeks group of pixels with uniform intensities. Seeded region growing performs a segmentation of an image with respect to set of points known as seed. Threat pixel generated from the above process can be considered as seed point. Given the seed the region growing method finds the tessellation of the image into regions with property that each connected component of region meets exactly one of Si. Each step of algorithm involves the addition of one pixel into above set. Let z be the unallocated pixel.

$$\alpha = \{x \Gamma Ui = 1 \text{ n } Si \,|n(x) \cap Ui = 1 \text{ n } Ai \neq \Phi\} \quad (3)$$

where, n(x) is set of immediate neighbours of the pixel neighbours of 8 connected pixel x. If x∈α then, n(x) meets just one of Ai. Hence, i(x)∈{1, 2, ..., n} to be the index such that:

$$n(X) \bigcap Si\ (X) \neq \Phi \quad (4)$$

$$\delta(X) = |g(X)\text{-mean } g \in Si\ (X)\ [g(y)]| \quad (5)$$

Where:

δ(X) = Measure of how different x is region it joins

g(x) = The gray value of the pixel x

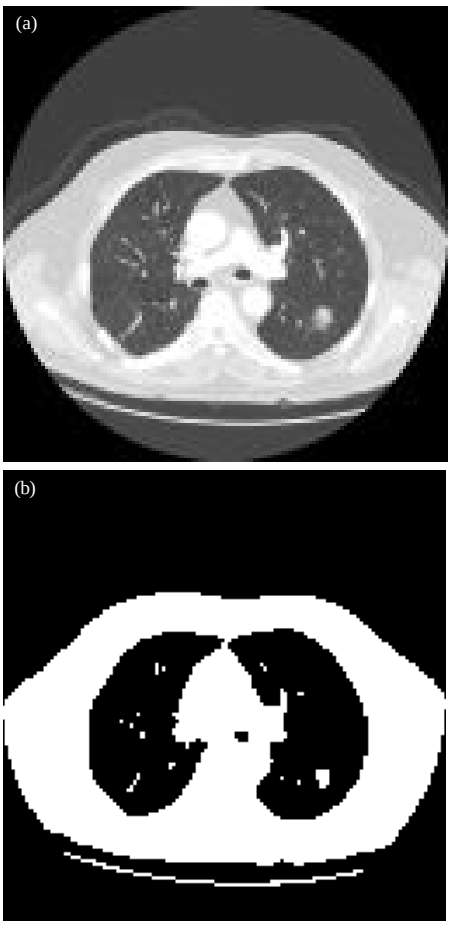

Fig. 3: a) The original image and b) the resultant image of segmentation

If N(x) meets two or more values of Ai then Ai will be selected according to the lowest value:

$$\delta(X) = \min x \in T\ \{\delta(X)\} \quad (6)$$

The process is repeated until all the threat pixels have been identified. Figure 3a shows the original image and 3b shows the resultant image of segmentation.

Feature extraction: After performing the segmentation, the features have to be extracted for detecting the cancer in the lung region correctly. This step concerns with two feature extraction such as Gray Level Co-occurrence Matrix (GLCM) and Gabor features. Texture feature is used in identifying normal and abnormal pattern. Texture is an alteration and variation of surface of the image. Texture is characterized as the space distribution of gray levels in neighborhood. A Gray Level Co-occurrence Matrix (GLCM) contains information about the positions

of pixels having similar gray level values. Texture descriptors derived from GLCM are contrast, energy, homogeneity and correlation:

$$\text{Contrast} = \sum_i \sum_j \frac{P_d[i, j]}{1+|i-j|} \quad (7)$$

$$\text{Homogeneit y} = \sum_{i=1}^{m}\sum_{j=1}^{n}|C(i, j)|\sum_i\sum_j (i-j)^k P_d[i, j]^n \quad (8)$$

$$\text{Energy} = \sum_{i=1}^{m}\sum_{j=1}^{n}|C(i, j)| \quad (9)$$

$$\text{Correlation} = \frac{\sum_i\sum_j [ijP_d[i, j]]-\mu_i\mu_j}{\sigma_i\sigma_j} \quad (10)$$

$$\text{Mean } (\mu_i) = \sum iP_d[i, j] \quad (11)$$

$$\text{Variance } (\sigma_i^2) = \sum i^2P_d[i, j]-\mu_i^2 \quad (12)$$

Where:

P(i, j) = Element i, j of the normalized symmetrical GLCM
N = Total number of gray levels in the image

- Contrast: measures the local variations in the gray-level co-occurrence matrix
- Homogeneity: measures the closeness of the distribution of elements in the GLCM to the GLCM diagonal
- Energy: provides the sum of squared elements in the GLCM. Also, known as uniformity or the angular second moment
- Correlation: measures the joint probability occurrence of the specified pixel pairs

The Gabor wavelets whose kernels are similar to the 2D receptive field profiles of mammalian cortical simple cells, exhibit desirable characteristics of spatial locality and orientation selectivity. Because Gabor wavelets capture the local structure corresponding to spatial frequency (scales), spatial localization and orientation selectivity (Schiele and Crowley, 2000), they are applied in many research areas widely such as texture analysis and image segmentation (Liu and Wechsler, 2002; Shen *et al*., 2007; Ferrari *et al*., 2001). Important activations can be extracted from the Gabor space in order to create a sparse object representation. The filter can be defined as:

$$\varphi(x, y; f, \theta) = \frac{f^2}{\pi\gamma\eta} e^{-\left(\frac{f^2}{\gamma^2}x'^2+\frac{f^2}{\eta^2}y'^2\right)} e^{j2\pi fx'^2} \quad (13)$$

$$x' = x\cos\theta + y\sin\theta \quad (14)$$

$$y' = -x\sin\theta + y\cos\theta \quad (15)$$

Where:

f = The central frequency of the sinusoidal plane wave
θ = The rotation angle of both the Gaussian major axis and the plane wave
γ = The sharpness along the major axis
η = The sharpness along the minor axis

The sharpness values along the major axis γ and along the minor axis η are set to 1. Image texture features can be extracted by convolving the image M(x, y) with Gabor filters:

$$g(x, y; f, \theta) = M \times \varphi(x, y; f, \theta) \quad (16)$$

Gabor filters with different frequencies fi and orientations θj are selected to obtain the texture features of the tumor area:

$$f(i) = 0.3 + 0.05i, \; i = 1, 2, ..., M \quad (17)$$

$$\theta j = \frac{j}{8}\pi \; j = 0, ..., 7 \quad (18)$$

where, M represents the number of selected Gabor filters (set to 20). After the image of the tumor area is convolved with Gabor wavelets with different frequencies and orientations, the extracted texture features, G are obtained as:

$$G = \{gij(x, y; fi, \theta j) | i = 1, ..., M; j = 0, ..., 7\} \quad (19)$$

where, gij (x, y; fi, θj) = ||M×φ (x, y; fi, θj)|| which is the magnitude of the Gabor filter response. By averaging the magnitude values of pixels of the tumor area over all directions, the different frequency features νj which represent the texture features of the tumor area are obtained:

$$V = (v1, ..., vi, ..., vN), i = 1, ..., N$$

where, V is the texture feature vector of the tumor area.

Classification: SVM (Gomathi and Thangaraj, 2010) is usually used for classification task which is introduced by Vapnik. For binary classification SVM is used to determine an Optimal Separating Hyper plane (OSH)

which produces a maximum margin between two categories of data. A transform that nonlinearly maps the data into a higher-dimensional space allows a linear separation of classes that cannot be linearly separated in the original space.

Theory of SVM is defined as: consider training set $D = \{(xj, yi)\}_{i=1}^{L}$ 1 with every input ni, $x \in R^n$ researchers have (f(x {w, b}) = sign (w.x+b). Also, an associated output $yi \in \{-1, +1\}$. Every input x is initially mapped into a higher dimension feature space F, by $z = \phi(x)$ through a nonlinear mapping ϕ: $R^n \rightarrow F$. If the data are linearly non-separable in F, then a vector $w \in F$ and a scalar b will exist which describe the separating hyper plane as:

$$y_i (w'.z_i + b) \geq 1-\xi_i, \forall i$$

where, $\xi(\geq 0)$ are knows as lack variable. The hyper plane that optimally splits the data in F is one that:

$$\text{minimize } ||w||^2 + C\sum_{i=1}^{m}{}_i$$

$$\text{subject to } y_i (w'.z_i + \beta) \geq -\xi_i, \quad \xi_i \geq 0, \forall i$$

where, C is knows as regularization parameter that finds the tradeoff between maximum margin and minimum classification error:

$$\text{Maximise } L(\alpha) = \sum_{i=1}^{n}\alpha_i - \frac{1}{2}\sum \alpha_i \alpha_j y_i y_j k(x_j, x_i)$$

$$\text{subject to } \sum_{i=1}^{L} y_i \alpha_i = 0, 0 \leq \alpha_i \leq C, \forall i$$

where, $\alpha_1, \ldots, \alpha_L$ represents the nonnegative lagrangian multipliers. The data points xi that corresponding to $\alpha_i > 0$ are considered as support vectors. In the proposed method RBF kernels are used:

$$k(x, x') = \exp(-||x-x'||/\sigma 2)$$

where, σ is positive real number. After completing the above process by using various constraints, the proposed method can able to detect normal, benign and malignant class in the lung region automatically.

RESULTS AND DISCUSSION

Experiments are carried out from real time datasets obtained from the reputed hospitals. Totally 11 patients are considered with 1 normal case, 2 benign cases and 8 malignant cases about 3278 sectional images. The 50% of dataset are considered for training and 50% as testing phases. The overall accuracy for the lung image 97.63% and the average false positives per scan is 2.13% which is better than the reported CAD System given in Table 1. Figure 4 shows sample results of Gabor filtered images. The four columns were Gabor filtered images corresponding to four orientations (0°, 45°, 90° and 135°). Some results of GLCM are given in Table 2.

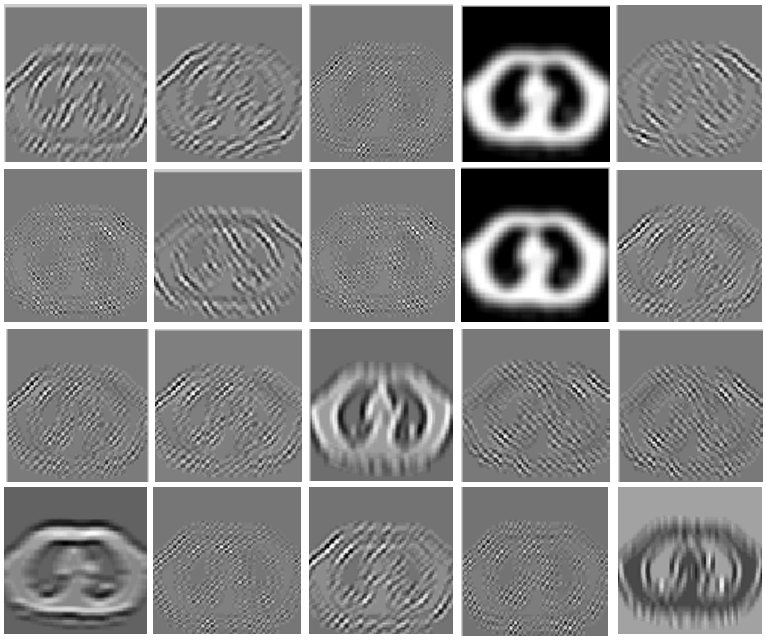

Fig. 4: Gabor filtered images for malignant class

Table 1: Some results of reported CAD System

CAD Systems	Nodule size (mm)	Sensitivity (%)	Avg. false positives/scan
Dehmeshki *et al.* (2007)	3-20	90.00	14.60
Suarez-Cuenca *et al.* (2009)	4-27	80.00	7.70
Messay *et al.* (2010)	3-30	82.66	3.00
Bellotti *et al.* (2007)	-	88.50	6.60
Choi and Choi (2012)	3-30	94.10	5.45
Proposed Method	3-30	100.00	2.13

Table 2: Result of feature extraction for normal, benign and malignant classes using GLCM

Test No.	Image class	Contrast	Homogeneity	Energy	Correlation
1	Normal	0.9662	0.8664	0.3752	0.9009
2	Benign	1.7624	0.8265	0.2432	0.8499
3	Benign	1.8250	0.8414	0.2488	0.8226
3	Malignant	0.5581	0.7965	0.9560	0.8357
4	Malignant	0.1531	0.9644	0.3252	0.9398
5	Malignant	0.1200	0.9712	0.3783	0.9542
6	Malignant	0.1344	0.9676	0.3118	0.9107
7	Malignant	0.2790	0.8947	0.3196	0.8997
8	Malignant	0.2492	0.8959	0.3475	0.9113
9	Malignant	0.2643	0.9191	0.3158	0.9161
10	Malignant	0.1350	0.9598	0.5141	0.9616
11	Malignant	0.2519	0.9234	0.3388	0.9205

CONCLUSION

In this study, automatic CAD System for detecting lung cancer nodules is proposed. It guarantees early detection of lung cancer nodules using computer tomography images. In the preprocessing step, lung region is been extracted. In the next step, segmentation is performed using threat pixel identification and region growing method. In the third step, features are extracted using GLCM and Gabor features. Finally, Support Vector Machines (SVM) is used for classification of normal, benign and malignant classes in the lungs. Experimental results show that the proposed system shows 100% of sensitivity.

ACKNOWLEDGEMENTS

Foremost, researchers would like to thank the almighty for the success in completing this research. Researchers would like to extend the thanks to all the reviewers for their critical comments.

REFERENCES

Abe, H., H. Macmahon, J. Shiraishi, Q. Li, R. Engelmann and K. Doi, 2004. Computer-aided diagnosis in chest radiology. Seminar Ultrasound CT MR., 25: 432-437.

Bellotti, R., F. De Carlo, G. Gargano, S. Tangaro and D. Cascio *et al.*, 2007. A CAD system for nodule detection in low-dose lung CTs based on region growing and a new active contour model. Med. Phys., 34: 4901-4910.

Choi, W.J. and T.S. Choi, 2012. Genetic programming-based feature transform and classification for theautomatic detection of pulmonary nodules on computed tomography images. Inform. Sci., 212: 57-78.

Dehmeshki, J., X. Ye, X. Lin, M. Valdivieso and H. Amin, 2007. Automated detection of lung nodules in CT images using shape-based genetic algorithm. Comput. Med. Imaging Graoh., 31: 408-417.

Dougherty, L., J.C. Asmuth and W.B. Gefter, 2003. Alignment of CT lung volumes with an optical flow method. Acad. Radiol., 10: 249-254.

Ferrari, R.J., R.M. Rangayyan, J.E.L. Desautels and A.F. Frere, 2001. Analysis of asymmetry in mammograms via directional filtering with Gabor wavelets. IEEE Trans. Med. Imaging, 20: 953-964.

Gomathi, M. and P. Thangaraj, 2010. A computer aided diagnosis system for lung cancer detection using support vector machine. Am. J. Applied Sci., 7: 1532-1538.

Howe, M.A. and B.H. Gross, 1987. CT evaluation of the equivocal pulmonary nodule. Comput. Radiol., 11: 61-67.

Hu, S., E.A. Hoffman and J.M. Reinhardt, 2001. Automatic lung segmentation for accurate quantization of volumetric X-ray CT images. IEEE Trans. Med. Imaging, 20: 490-498.

Kim, H., T. Nakashima, Y. Itai, S. Maeda, J.K. Tan and S. Ishikawa, 2007. Automatic detection of ground glass opacity from the thoracic MDCT images by using density features. Proceedings of the International Conference on Control, Automation and Systems, October 17-20, 2007, Seoul, Korea, pp: 1274-1277.

Lee, Y., T. Hara, H. Fujita, S. Itoh and T. Ishigaki, 2001. Automated detection of pulmonary nodules in helical CT images based on an improved template-matching technique. IEEE Trans. Med. Imaging, 20: 595-604.

Liu, C. and H. Wechsler, 2002. Gabor feature based classification using the enhanced fisher linear discriminant model for face recognition. Image Proc. IEEE Trans., 11: 467-476.

Messay, T., R.C. Hardie and S.K. Rogers, 2010. A new computationally efficient CAD system for pulmonary nodule detection in CT imagery. Med. Image Anal., 14: 390-406.

Okada, K., D. Comaniciu and A. Krishnan, 2005. Robust anisotropic Gaussian fitting for volumetric characterization of pulmonary nodules in multislice CT. IEEE Trans. Med. Imaging, 24: 409-423.

Parveen, S.S. and C. Kavitha, 2012. A review on computer aided detection and diagnosis of lung cancer nodules. Int. J. Comput. Technol., Vol. 3.

Penedo, M.G, M.J. Carreira., A. Mosquera and D. Cabello, 1998. Computer-aided diagnosis: A neural-network-based approach to lung nodule detection. IEEE Trans. Med. Imaging, 17: 872-880.

Pohle, R. and K.D. Toennies, 2001. Segmentation of medical images using adaptive region growing. Proc. SPIE Medical Imaging, 4322: 1337-1346.

Schiele, B. and J.L. Crowley, 2000. Recognition without correspondence using multidimensional receptive field histograms. Int. J. Comput. Vis., 36: 31-50.

Shen, L., L. Bai and M. Fairhurst, 2007. Gabor wavelets and general discriminant analysis for face identification and verification. Image Vision Comput., 25: 553-563.

Sluimer, I., M. Prokop and B. van Ginneken, 2005. Toward automated segmentation of the pathological lung in CT. IEEE Trans. Med. Imaging, 24: 1025-1038.

Song, Y., W. Cai, J. Kim and D.D. Feng, 2012. A multistage discriminative model for tumor and lymph node detection in thoracic images. IEEE Trans. Med. Imaging, 31: 1061-1075.

Suarez-Cuenca, J.J., P.G. Tahoces, M. Souto, M.J. Lado, M. Remy-Jardin, J. Remy and J.J. Vidal, 2009. Application of the iris filter for automatic detection of pulmonary nodules on computed tomographyimages. Comput. Biol. Med., 39: 921-933.

Suzuki, K., H. Abe, H. MacMahon and K. Doi, 2006. Image-processing technique for suppressing ribs in chest radiographs by means of Massive Training Artificial Neural Network (MTANN). IEEE Trans. Med. Imaging, 25: 406-416.

Ye, X., X. Lin, J. Dehmeshki, G. Slabaugh and G. Beddoe, 2009. Shape-based computer-aided detection of lung nodules in thoracic CT images. IEEE Trans. Biomed. Eng., 56: 1810-1820.

Yim, Y., H. Hong and Y.G. Shin, 2005. Hybrid lung segmentation in chest CT images for computer-aided diagnosis. Proceedings of 7th International Workshop on Enterprise Networking and Computing in Healthcare Industry, June 23-25, 2005, Busan, Korea, pp: 378-383.